

## EFFICIENCY OF IMAGE CORRECTION WHEN COMPENSATING FOR RANDOM WAVE-FRONT TILT ANGLES OF RADIATION PASSED THROUGH THE TURBULENT ATMOSPHERE

L.V. Antoshkin, N.N. Botygina, O.N. Emaleev, and V.P. Lukin

*Institute of Atmospheric Optics,  
Siberian Branch of the Russian Academy of Sciences, Tomsk  
Received May 25, 1995*

*Reported in this paper are the results of our investigation into the efficiency of correction for the distortions caused by atmospheric turbulence when image of a laser beam is formed with an adaptive optical system having closed contour of control over the total and local wave-front tilts when tracking over angular displacement of the whole image and its quadrants. It is shown in particular that the use of a segmented mirror with controllable tilt angles as a corrector improves the quality of imaging under conditions of strong turbulence.*

To correct an image whose distortions are caused by the atmospheric turbulence we have already proposed<sup>1</sup> an adaptive optical system with open contour of control over total wave-front tilts. The main disadvantages of such systems are strict requirements for linearity and accuracy of instrumentation, unfeasibility to compensate for control errors caused by incomplete account of external perturbations and instability (drift) of the characteristics of controllable mirror. A system with closed control contour is free from the above disadvantages.

In this paper, we present the results of our investigation into the efficiency of image correction with an adaptive optical system having closed contour of control over total and local of wave-front tilts when tracking over angular displacement of the whole image and its quadrants.

### DESCRIPTION OF EXPERIMENTAL SETUP

Block diagram of experimental setup is shown in Fig. 1. The radiation from the helium-neon LGN-222 laser 1 was collimated with the two-component lens system 2. The propagation of laser beams with the Fresnel parameters  $\Omega_s = 18.2$  and  $1.44$  was investigated on the atmospheric path 3 of length  $L$  being equal to 100 m at 10 m altitude above the underlying surface. The measurements were conducted with the Fresnel parameters of the input aperture  $\Omega_t = 3, 0.75,$  and  $0.4$ . Hereinafter, we use the following designations:  $\Omega_s = ka_0^2/L$ ,  $\Omega_t = ka_t^2/L$ , where  $k$  is the wave number,  $a_0$  is the beam radius at the level  $e^{-1}$ ,  $a_t$  is the effective radius of the input aperture in the Gaussian representation of the lens transmission function. The maximum radius of the input aperture was determined by the size of the bimorph deflector 5 being controlled

over the tilt angles in perpendicular planes.<sup>2</sup> The deflector sensitivity in the 0–190 Hz frequency band was equal to  $1.08 \cdot 10^{-6}$  rad/V in horizontal plane and  $1.26 \cdot 10^{-6}$  rad/V in vertical plane. The frequencies of mechanical resonance were  $f_1 = 260$  Hz (resonance contour quality factor  $Q = 2.5$ ) and  $f_2 = 400$  Hz ( $Q = 2.5$ ) in horizontal plane and  $f_1 = 280$  Hz ( $Q = 2.5$ ) and  $f_2 = 400$  Hz ( $Q = 6$ ) in vertical plane.

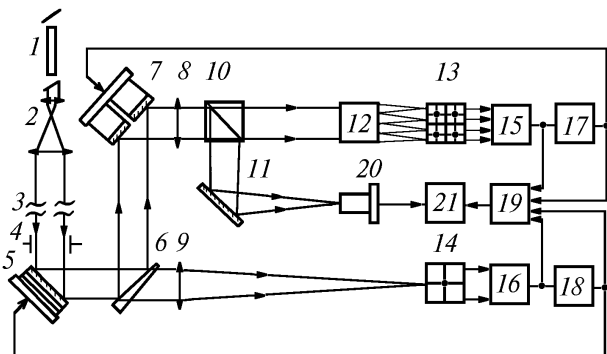


FIG. 1. Block diagram of experimental setup: helium-neon LGN-222 laser (1), collimator (2), atmospheric path 100 m long (3), iris of variable radius (4), bimorph deflector (5), beam-splitting optical wedge (6), four-element controllable mirror (7), objectives of focal length of 1600 mm (8 and 9), beam-splitting cube (10), folding mirror (11), image divider into quadrants (12), matrix of photodetectors (13), individual FD-19KK quadrant position-sensitive photodetector (14), X-Y recorders of angular displacements of image centroid (15 and 16), control units (17 and 18), eight-channel histogram (19), KT-8 TV camera (20), and personal computer (21).

The local wave-front tilts were controlled with the four-element segmented mirror 7. As pushers we used hollow cylinders made of TTS-19 piezoceramic with electrodes divided into four parts on the inside and outside. The controlling voltages were fed to electrodes in such a way that to provide the tilts of an individual mirror element about orthogonal axes. The design of segmented mirror provides for mechanical adjustment of its elements. An analysis of influence of the design features upon dynamic characteristics of segmented mirror allowed us to create the construction with optimal distribution of moving masses and optimal stiffness of constructional element joints. The frequency of the first mechanical resonance of an individual mirror element was 4.0 kHz ( $Q = 7$ ) in horizontal plane and 3.9 kHz ( $Q = 9$ ) in vertical plane. In 0–2 kHz bandwidth the sensitivity was  $2.83 \cdot 10^{-7}$  rad/V for tilts about horizontal axis and  $2.46 \cdot 10^{-7}$  rad/V for tilts about vertical axis.

The image was formed by the objectives 8 and 9 with focal length  $F = 1600$  mm. In the focal plane of objectives 8 and 9, the FD-19KK quadrant position-sensitive photodetector 14 and the matrix 13 composed of four FD-19KK photodetectors were placed. Two pairs of plane-parallel plates oriented at an angle to each other were used as image divider 12. Arrangement of pairs of plates provided the required displacement of image quadrants in accordance with the position of detectors in the matrix 13.

On the basis of comparison of radiant flux distribution over the quadrants of photodetectors in measurement units 15 and 16 (Ref. 1), signals were generated proportional to angular displacement of the centroid of the whole image and its quadrants. The signals were fed into the control units 17 and 18, where they were processed according to the control law, and then were fed into the piezoelectric actuators of the adaptive mirrors 5 and 7.

To analyze random signals coming from the control units and the recorders of angular displacements of image, the 8-bit histogrammatom built around the personal computer 21 was used.

The corrected image with the help of the beam-splitting cube 10 and the mirror 11 was transferred in the plane of recording. To display the image on a video control device and to enter it into the IBM-compatible personal computer 21 with special-purpose interface plate, the modified KT-8 TV camera 20 was used built around the CCD matrix K1200TM7B. The TV camera field of view was  $670 \times 930 \mu\text{m}$ , the number of pixels was  $256 \times 256$ , and the number of pixel levels was 64.

## TRACKING SYSTEM

When selecting the structure of the system of automatic control to compensate for angular displacement of image, we took into account that for separation of valid signal against the background of

noise in the case in which both signals at the system input are uncorrelated random processes, the transfer function corresponding to a smoothing device of the integrator type is optimal.<sup>3</sup> Figure 2 shows the block diagram of the tracking system, where Roman number I denotes the tracking system of compensation for image angular displacements in control over the total wave-front tilts, Roman number II denotes the four-channel tracking system of compensation for image angular displacements in control over local wave-front tilts,  $\alpha$  and  $\alpha_i$  are the angular displacements of the centroid of the whole image and its  $i$ th sector caused by atmospheric turbulence ( $i = 1, 2, 3, 4$ ),  $\alpha_0$  and  $\alpha_{0i}$  are the angular displacements of the centroid of the whole image and its  $i$ th sector by controllable mirrors,  $\varepsilon = \alpha - \alpha_0$  and  $\varepsilon_i = \alpha_i - \alpha_{0i}$  are the errors of control. Enumerated in Fig. 2 are the recorder of angular displacements of the centroid of image based on the quadrant photodetector 1, the integrator based on the operational amplifier 2, the high-voltage amplifier<sup>4</sup> 3, and the controllable mirror 4.

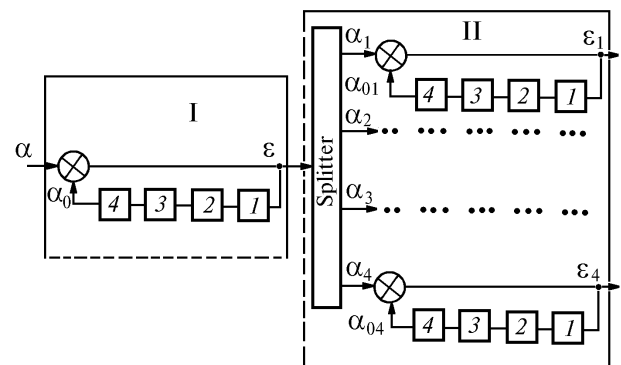


FIG. 2. Block diagram of the system of automatic control.

System parameters were calculated from the requirements for the reserve of stability providing fast decay and small oscillations of transient process. Frequency methods with the use of logarithmic frequency characteristics provided a basis for calculations. To ensure the desired quality of the transient process and to take into account the random character of a signal with *a priori* unknown spectrum entering the tracking system, the feasibility to change the gain of the system in adjustment mode was provided.

Shown in Fig. 3 are the logarithmic amplitude-frequency characteristics  $L(\omega)$  of open circuit of the system of compensation for image angular displacements along the  $Y$  axis in control over total (a) and local (b) wave-front tilts (Fresnel parameter of the source  $\Omega_s = 18.2$  and of the input aperture  $\Omega_t = 30$ ):

$$L(\omega) = 20 \log \frac{k_1 k_2 k_3 k_4}{\sqrt{(1 + k_2^2 T_1^2 \omega^2)[(1 - \omega^2 T_2^2)^2 + \omega^2 T_1^2]}}, \quad (1)$$

where  $k_1$  is the slope of the positional characteristic of the recorder,  $k_2$  is the gain of the operational amplifier,  $T_i$  is the time constant of the integrator,  $k_3$  is the gain of the high-voltage amplifier,  $k_4 = 2S$  ( $S$  is the slope of the static characteristic of the controllable mirror),  $T_2$  and  $T_1$  are the time constants of the controllable mirror,  $T_2 = 1/\omega_{res}$ ,  $\omega_{res}$  is the resonance frequency, and  $T_2/T_1 = Q$  is the quality factor of resonance contour of the controllable mirror.

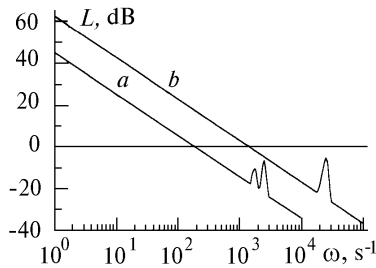


FIG. 3. Amplitude-frequency characteristic of the tracking system in the control over total wave-front tilts (a) and local wave-front tilts (b).

The quality of tracking process can be evaluated from the form of the logarithmic amplitude-frequency characteristic. Table I presents the parameters of the tracking system with different Fresnel parameters of the receiving aperture: total gain of the open circuit  $K$ , minimum frequency  $\omega_1$  of the frequency band of an input signal being reconstructed by the tracking system practically without distortions ( $\epsilon_{max}/\alpha_{max} = 1/[1 + |W(\omega_1)|] = 3\%$ , where  $W(\omega_1)$  is the transfer function of the open circuit,  $L(\omega_1) = 30$  dB), cutoff frequency  $\omega_c$  ( $L(\omega_c) = 0$ ) which characterizes the rate of the transient process decay, reserve of stability in amplitude and resonance frequency  $L(\omega_{res})$ .

TABLE I.

Parameters	$\Omega_s = 18.2, \Omega_t = 3.0$				$\Omega_s = 18.2, \Omega_t = 0.75$			
	Control over tilts							
	Total		Local		Total		Local	
	X	Y	X	Y	X	Y	X	Y
$K$	171	178	1977	1328	188	213	1610	823
$\omega_1, s^{-1}$	5.4	5.6	62.5	42	5.9	6.7	51	26
$\omega_c, s^{-1}$	171	178	1977	1328	188	213	1610	823
$L(\omega_{res})$	-8.1	-7.4	-5.2	-6.3	-7.3	-5.9	-7	-10

An attempt to improve the precision and dynamic characteristics of the system due to introduction of correcting devices with preset parameters of controllable mirrors led to no essential improvement in tracking quality and it was recognized that there is no point in complicating the system with additional elements.

MEASUREMENT TECHNIQUE AND RESULTS

Measurements were conducted for three modes of the tracking system operation: in control over total wave-front tilts of radiation, over local tilts, and in simultaneous control over total and local wave-front tilts. Mean diffraction pattern in the focal plane of the receiving lens was analyzed.

The turbulent state of the atmosphere on the path of radiation propagation was characterized by the structural constant of the refractive coefficient  $C_n^2$ , derived from the measured variance of image jitter in the focal plane of the lens  $\sigma_t^2$ . For calculation of  $C_n^2$ , we used the following expression<sup>5</sup>:

$$\sigma_t^2 = \pi^2 0.033 F^2 L C_n^2 \Gamma(1/6) (a_t^2/2)^{-1/6} [1 + S(\Omega_t)], \tag{2}$$

$$S(\Omega_t) = \int_0^1 \text{Re}[(1 + i \Omega_t^{-1} \xi)^{-1/6}] d \xi .$$

The values of function  $S(\Omega_t)$  were found by numerical integration (by the trapezoid rule) with a relative error of  $10^{-4}$ . To provide the operation of the recorder of image angular displacements in linear section of its positional characteristic, the diameter of the receiving aperture was decreased down to 8 mm ( $\Omega_t = 0.40$ ) when measuring  $C_n^2$ . The measurements were carried out with  $\Omega_s = 18.2$ . The variance was estimated from the histogram. Discretization frequency in histogram collecting was 870 Hz for 5 min time of realization.

When obtaining the mean diffraction pattern, uncorrelated samples with a sampling frequency of 0.25 Hz and sample size of 200 video frames were used. Video frame exposure lasted 20 ms.

In the process of accumulation of mean diffraction pattern, histograms of control and error signals were collected to monitor the following relative errors of

control:  $\epsilon' = \frac{\sigma_\epsilon}{\sigma_{\alpha_0}}$  in the mode of control over total

wave-front tilts,  $\epsilon_i'' = \frac{\sigma_{\epsilon_i}}{\sigma_{\alpha_{0i}}}$  in the mode of control over

local tilts, and  $\epsilon''' = \frac{\sigma_\epsilon}{\sigma_{\alpha_0}}, \epsilon_i''' = \frac{\sigma_{\epsilon_i}}{\sigma_{\alpha_{0i}}}$  in simultaneous

control over total and local wave-front tilts.

The quality of image correction was evaluated from the energy distribution over the mean diffraction pattern. To this end, the energy fraction  $E$  in a circle of preset radius was calculated.

Figure 4 shows this value as a function of radius of the mean diffraction pattern for different levels of turbulence and different Fresnel parameters of emitting and receiving apertures.

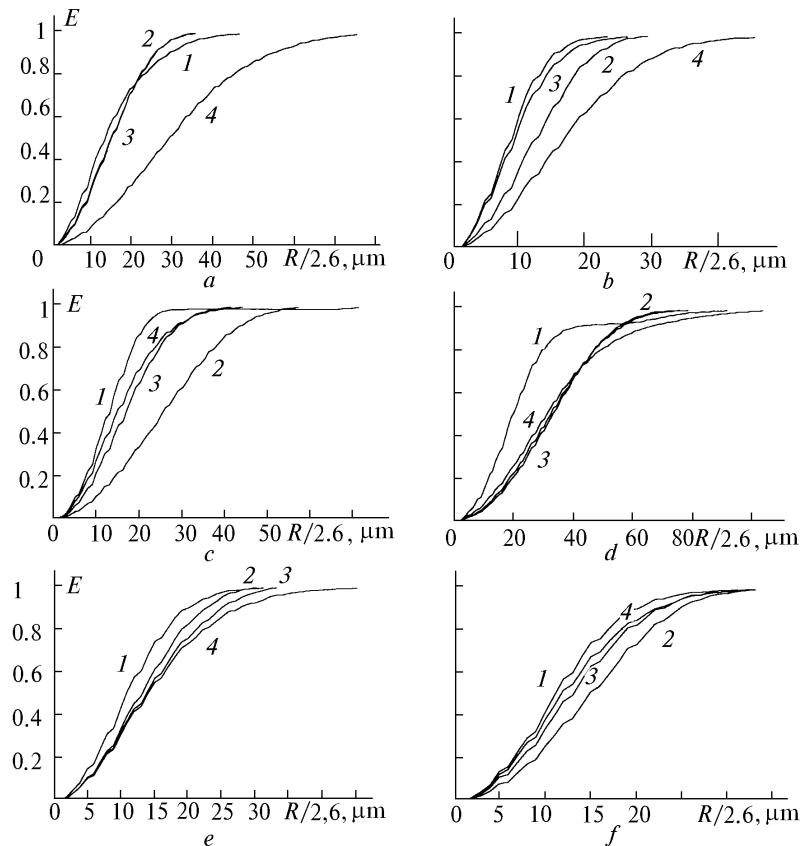


FIG. 4. Efficiency of image correction. Energy distribution in the mean diffraction pattern in control over total tilts (curve 1), over local tilts only (curve 2), in simultaneous control over both local and total tilts (3), and without any correction (4):  $\Omega_s = 18.2$ ,  $\Omega_t = 3$ ,  $C_n^2 = 3.6 \cdot 10^{-14} \text{ cm}^{-2/3}$ ,  $\epsilon' = 8.2\%$ ,  $\langle \epsilon_i'' \rangle = 1.0\%$ ,  $\epsilon''' = 5.6\%$ ,  $\langle \epsilon_i''' \rangle = 1.3\%$  (a);  $\Omega_s = 18.2$ ,  $\Omega_t = 3$ ,  $C_n^2 = 8.7 \cdot 10^{-15} \text{ cm}^{-2/3}$ ,  $\epsilon' = 10.3\%$ ,  $\langle \epsilon_i'' \rangle = 1.2\%$ ,  $\epsilon''' = 6.3\%$ ,  $\langle \epsilon_i''' \rangle = 1.9\%$  (b);  $\Omega_s = 18.2$ ,  $\Omega_t = 0.75$ ,  $C_n^2 = 8.7 \cdot 10^{-15} \text{ cm}^{-2/3}$ ,  $\epsilon' = 12.1\%$ ,  $\langle \epsilon_i'' \rangle = 4.3\%$ ,  $\epsilon''' = 15.3\%$ ,  $\langle \epsilon_i''' \rangle = 10\%$  (c);  $\Omega_s = 18.2$ ,  $\Omega_t = 0.75$ ,  $C_n^2 = 1.5 \cdot 10^{-14} \text{ cm}^{-2/3}$ ,  $\epsilon' = 9.1\%$ ,  $\langle \epsilon_i'' \rangle = 1.0\%$ ,  $\epsilon''' = 6\%$ ,  $\langle \epsilon_i''' \rangle = 1.5\%$  (d);  $\Omega_s = 1.44$ ,  $\Omega_t = 3$ ,  $\sigma_\alpha^2 = 8.3 \cdot 10^{-11}$  (e);  $\Omega_s = 1.44$ ,  $\Omega_t = 3$ ,  $\sigma_\alpha^2 = 4 \cdot 10^{-10}$  (f).

With  $\Omega_s > \Omega_t$  under conditions of significant turbulent distortions of image (Fig. 4a) the control over total wave-front tilts results in a higher degree of energy concentration in the image center; however, total energy turns out to be concentrated in a circle of a radius greater than that in control over local tilts. The latter may be connected with the fact that a tracking error in control over total wave-front tilts is greater than that in control over local tilts.

For weaker distorting effect of turbulence and the same Fresnel parameters (Fig. 4b), the control over total wave-front tilts is more efficient than that over local tilts and the simultaneous control over both local and total tilts.

Decrease of the input aperture (Fig. 4c) results in the deterioration of the mean diffraction pattern in the control over local wave-front tilts and in the simultaneous control over both total and local tilts.

For stronger turbulence (Fig. 4d) the control over local tilts leads to decrease of size of the mean diffraction pattern, but the degree of energy concentration in the center of pattern turns out to be lower than that in uncorrected image.

In the case of a narrow beam propagating in the atmosphere, when the Fresnel parameter of emitting aperture is  $\Omega_s = 1.44$  and that of receiving aperture is  $\Omega_t = 3$ , the control over local tilts results in deterioration of the mean diffraction pattern for weak atmospheric turbulence (Fig. 4f) and in slight improvement of the energy distribution in the mean diffraction pattern for stronger atmospheric turbulence (Fig. 4e).

The control over total wave-front tilts in all cases results in image improvement.

## DISCUSSION OF RESULTS AND CONCLUSIONS

The results of investigation into the efficiency of image correction shown in Figs. 4a–d correspond to the experimental situation when the mean beam radius  $a_b$  in the plane of receiving lens far exceeds the lens radius  $a_{\text{lens}}$ . For a collimated beam,<sup>5</sup>  $a_b = a_0 [1 + \Omega_s^{-2} (1 + 4/3 a_0^2 / \rho_p^2)]^{1/2}$ , where  $\rho_p$  is the coherence radius of a plane wave. With  $a_b > a_{\text{lens}}$ , the effective pupil radius  $a_{\text{eff}} = [1/a_b^2 + 4/a_{\text{lens}}^2]^{-1/2}$  is primarily governed by the radius of the receiving lens. Then the

radius of mean diffraction pattern in the focal plane of the lens is  $R_m \sim F/k [4/\rho_c^2 + 4/a_{\text{lens}}^2]^{1/2}$  (where  $\rho_c$  is coherence radius of beam), since under the conditions of our experiment the mean radius of the image in the geometrical-optics approximation was far smaller than the mean radius of the diffraction image.

The segmented mirror with each element being clamped at its center and controlled over the angle undergoes dephasing in the process of control; therefore, the minimum size of an image in the focal plane of receiving lens is limited by the diffraction on an individual mirror element. Efficiency of image correction in control over local wave-front tilts depends on the relation between the size of diffraction image of an individual subaperture and the radius of the mean diffraction pattern whose distortions are caused by atmospheric turbulence. The control over local tilts, when the inequality  $2/a_{\text{el}} < [4\rho_c^2 + 4/a_{\text{lens}}^2]^{1/2}$  or  $a_{\text{el}} > \rho_c(M - 1/M)^{1/2}$  (where  $a_{\text{el}}$  is the size of an individual element of the segmented mirror, and  $M$  is the number of elements) is valid, results in image improvement (Figs. 4a and b). Otherwise, the control over local tilts leads to the deterioration of the diffraction pattern (Fig. 4c).

When a narrow laser beam is propagated, the quality of image correction due to compensation for local tilts improves, if the size of image of illuminated parts of subapertures in non-cophased summation in the focal plane is less than the radius of the mean diffraction pattern  $R_m \sim F/k [4/\rho_c^2 + 4/a_{\text{lens}}^2 + 1/a_b^2]^{1/2}$ . Under conditions of our measurements for atmospheric turbulence corresponding to the value of the parameter  $q < 0.72$  ( $q = L/k\rho_p^2$ ), the control over total wave-

front tilts against the selected criterion of image quality was more efficient than the control over local tilts.

The use of the segmented mirror controllable only in tilt angles as a corrector improves the image under conditions of strong turbulence, but for weak atmospheric turbulence it may result in deterioration of the mean diffraction pattern.

#### ACKNOWLEDGMENTS

We would like to acknowledge L.N. Lavrinova, P.A. Konyaev, and A.P. Rostov, who put at our disposal the software for processing of measurement results, and A.P. Yankova for technical help.

The work was supported in part by the Russian Fundamental Research Foundation Grant No. 94-03027a and International Science Foundation Grant No. NY 1000.

#### REFERENCES

1. L.V. Antoshkin, N.N. Botygina, O.N. Emaleev, V.P. Lukin, and S.F. Potanin, *Atm. Opt.* **2**, No. 6, 510-514 (1989).
2. L.V. Antoshkin, O.N. Emaleev, and V.P. Lukin, *Prib. Tekhn. Eksp.*, No. 5, 211-212 (1988).
3. V.A. Bessekerskii, *Dynamic Synthesis of Systems for Automatic Control* (Nauka, Moscow, 1970), 575 pp.
4. L.V. Antoshkin, *Atmos. Oceanic Opt.* **5**, No. 12, 850-851 (1992).
5. V.E. Zuev, V.A. Banakh, and V.V. Pokasov, *Optics of the Turbulent Atmosphere* (Gidrometeoizdat, Leningrad, 1988), 270 pp.